Polymer Degradation in Porous Media Flow

RAYMOND S. FARINATO and WEI S. YEN, *Stamford Research Laboratories, American Cyanamid Co., Stamford, Connecticut 06904*

Synopsis

The hydrodynamic degradation of high molecular weight poly(acrylamide-co-Na acrylate) in 1*M* NaCl in porous media flow was studied as a function of polymer concentration in the dilute and semidilute concentration ranges. Porous media rheometry was used to monitor molecular weight changes due to chain scission. At equivalent superficial velocities of flow through a glass bead pack, polymers at dilute concentrations showed greater loss of molecular weight than polymers at semidilute concentrations.

INTRODUCTION

The coil-stretch transition of solvated flexible macromolecules in elongational flow fields underlies both the excess pressure drops associated with viscoelastic polymer fluid flow through porous media and the hydrodynamic degradation of the macromolecules via main chain scission. The dynamics of flexible macromolecules undergo significant changes as the polymer concentration passes through different regimes.[1] This is governed by the relative importance of intra- and intermolecular polymer interactions. This concentration dependence is well documented.[2-5] Recently, quantitative predictions of the concentration dependence of polymer relaxation times in the dilute and semidilute regimes using the perturbation approach have been carried out by Muthukumar[6] and Muthukumar and Freed.[7] These predictions were in good agreement with polymer solution dynamics measured by Martel et al.[8] and Lodge et al.[9]

The factors affecting hydrodynamic degradation of polymer solutions have been widely investigated. Experiments have been reported for a variety of flow situations with varying degrees of flow complexity. The more difficult flows to analyze have included those in high speed blenders[10-13] and other configurations where turbulence was significant. Careful experiments in concentric cylinders,[14-17] capillaries,[18-20] converging tubes and constricted passages,[21-23] crossed slots,[24] and porous media[25-29] have shown that, by far, the major damage done to flexible polymers occurs in regions where elongational flow dominates. The various factors influencing hydrodynamic degradation include parameters that influence the flow field (e.g., flux, porosity and particle size in a porous medium) and parameters that characterize the macromolecules (e.g., carbon–carbon bond strength, intramolecular interactions, and hydrodynamic size).

Our interest was in how polymer concentration affected degradation in porous media, especially in going from the dilute into the semidilute concentration regime. It is this range of concentrations which is important, for example, in applications of high molecular weight water-soluble polymers to

Journal of Applied Polymer Science, Vol. 33, 2353–2368 (1987)
 CCC 0021-8995/87/072353-16$04.00

enhanced oil recovery. Since the polymer dynamics were significantly effected by the intermolecular interactions that arise in the semidilute concentration regime, a significant effect on polymer degradation was expected as well.

Macromolecular scission in dilute solutions in extensional flow has been shown to proceed by a chain-halving mechanism.[22,24,30] The tensile forces necessary for chain rupture are in good agreement with the force necessary for carbon–carbon bond rupture. As for the effect of polymer concentration, Merrill and Horn[22] reported a monotonic increase in the degree of degradation of dilute solutions of 0.9 megadalton polystyrene in cyclohexane as the concentration decreased from 500 to 5 ppm. In a study of porous media degradation of a high molecular weight (5–7 megadaltons) partially hydrolyzed polyacrylamide in aqueous salt solutions, Maerker[25,26] reported that mechanical degradation was not affected by polymer concentration over a narrow range (300–600 ppm). Morris and Jackson[31] showed that increasing the polymer concentration up to 2000 ppm of polyacrylamide decreased the amount of degradation in porous media flow.

In this work we have taken a systematic look at the degradation of hydrolyzed polyacrylamide (HPAM) in porous media flow as a function of polymer concentration going from the dilute into the semidilute regime. Porous media flow, even for regularly packed geometries, is a combination of shear and elongational flows. This pertains even in the absence of turbulence. Secondary and unsteady flows also contribute and can dominate the flow patterns for viscoelastic liquids above certain Reynolds numbers. Visualizations of these patterns have been captured by many investigators in both porous media flow[32] and other similar geometries where elongational flow was evidenced.[33–35]

Theoretical treatments of porous media flow attempt to separate viscoelastic from viscometric effects.[36,37] Non-Newtonian laminar fluid flow in packed beds can be modeled, excluding viscoelastic effects, with a capillary flow model combined with a particular rheological model to give a modified Ergun equation.[38] We have chosen to use the Ellis fluid model[39] for our data since this gave the best fit to our viscometric data (concentric cylinder) on these fluids. Duda[40] have pointed out the inadequacies of the conventional capillary models, but these adjustments can be considered small when compared to the viscoelastic effects at Reynolds numbers where the coil-stretch transition is important.

Viscoelastic effects appear at a critical value of the Deborah number, De, (ratio of the time scales of the material and the flow process). Because of a hysteresis in the coil-stretch transition[41] in converging/diverging flow geometries, the macromolecules stretch faster than they relax. This allows a cumulative stretching effect to take place in periodic porous media,[42,43] and hence the importance of the Deborah number for predicting the stretching transition onset. In porous media flow these viscoelastic effects are manifested as an excess pressure drop above that calculated from a modified Ergun equation. Above the onset Reynolds number, Re_o, these viscoelastic effects can surpass the viscometric flow effects by several orders of magnitude. The viscoelastic effects in porous media flow have been associated with macromolecular stretching and not necessarily secondary flows.[42,44,45]

The extensional viscosity calculated from a kinetic theory of dilute solutions of finitely extensible, nonlinear elastic (FENE) dumbbells[46–48] has been

shown to be in good agreement with experiments on flexible polymer solutions in porous media flow.[48-50] This has established the use of porous media rheology as a method of indirectly determining the molecular weight of extremely high molecular weight flexible polymers.[51] We have used this kind of methodology to monitor molecular weight changes as a result of hydrodynamic degradation in porous media flow. Thus our porous medium is used both as a locus for degradation and as a rheometer.

EXPERIMENTAL

Porous Media Rheometer

A schematic of the flow experiment is shown in Figure 1 and a diagram of the porous media rheometer in Figure 2. The porous medium consisted of well characterized glass beads housed in a cylindrical stainless steel chamber. The pressure drop across an internal length of the bead pack was measured with a Validyne differential pressure transducer (Validyne Engineering, Northridge, CA) calibrated with a manometer. Under flow conditions where pressure fluctuations were encountered the average pressure from a ΔP versus t record was determined. The sized glass beads (#P0230) were made of soda-lime silica glass from Potter Industries (Hasbrouck Heights, NJ). The beads had an average diameter, D_p, of 590 μm as determined from applying the Blake-

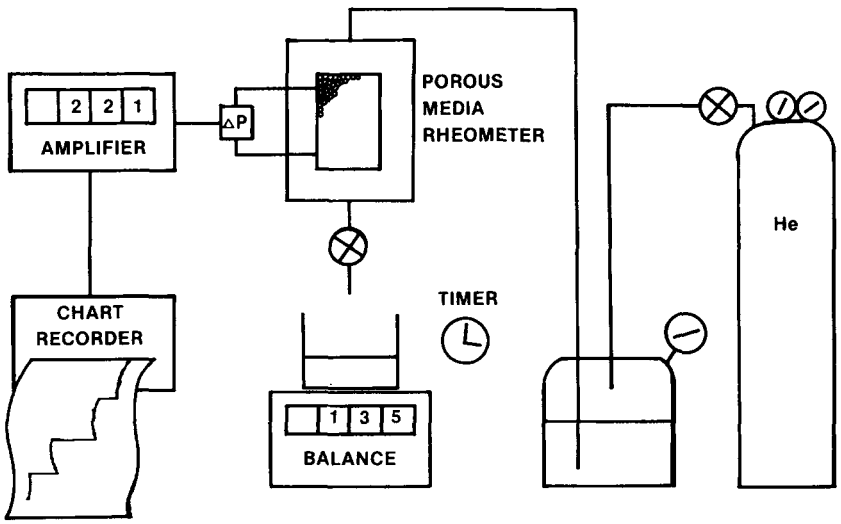

Fig. 1. Porous media rheometer.

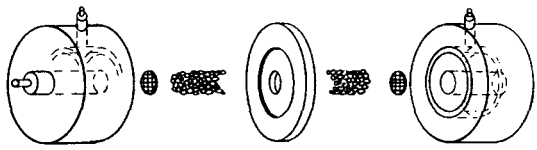

Fig. 2. Porous media rheometer; detail of flow cell.

Kozeny-Carman equation:[52]

$$k = \frac{D_p \phi^3}{180(1 - \phi)^2} \tag{1}$$

to pressure drop-flow rate data for $1M$ NaCl. The void fraction, ϕ, was typically 0.34. The permeability, k, of the bead pack to $1M$ NaCl was typically ~ 200 darcies and was regularly monitored for changes. Throughout any one set of experiments, k remained constant to within 5%. Bead packs were preconditioned by passing through them ~ 1000 pore volumes of polymer solution before using. Preflushing between polymer solutions in the same series was typically with 10–20 pore volumes. All measurements were done at room temperature, $T = 22 \pm 2°C$. Pulseless flow was accomplished using a stainless steel reservoir (Amicon, Danvers, MA) pressurized with helium. A certain number of pore throat units needed to be traversed before a steady state of polymer elongation was reached. Haas and Durst[47] showed that maximum stretching of an HPAM occurred after about 4 contractions in a regularly packed bed of spheres, though further changes in the f versus Re profile did not stabilize (around Re_o) until > 8 contractions. Chauveteau,[42] using periodic contraction elements of concentric capillaries, showed that Re_o was not strongly dependent on the number of elements, but that the details of the f versus Re curve were dependent on the number of elements. We designed our packed bed so that the polymer solution flowed through at least 30 bead diameters before the pressure drop was measured.

Flow Experiments

The bead pack was used in two modes: as a rheometer and as a locus for degradation. In the rheometer mode, when the fluids were not reused, the flow rate was regulated by maintaining a constant reservoir pressure and adjusting a needle valve at the outlet. In the degradation mode, the flow rate was regulated by the helium pressure in the reservoir.

In the rheometer mode the polymer solutions were flowed through the bead pack at low to intermediate rates, normally below the Reynolds number where degradation became evident. Steady-state pressure drops, ΔP, over an $L = 0.58$ cm section approximately 2 cm from the entrance face were measured along with a gravimetric determination of the flow rate. Using the polymer solution density this was converted into a volumetric flow rate, Q. The friction factor,

$$f = \frac{\Delta P D_p \phi^3}{L \rho v^2 (1 - \phi)} \tag{2}$$

and Reynolds number,

$$\mathrm{Re} = \frac{D_p \rho v F}{(1 - \phi)\eta_{\mathrm{eff}}} \tag{3}$$

were computed for a polymer solution of density ρ and effective viscosity η_{eff}.

The effective viscosity was computed for an Ellis fluid model[38] from viscometric data taken on a Haake RV100/CV100 low shear rheometer (Haake Buchler Inc., Saddle Brook, NJ) at 25.0°C.

$$\eta_{\text{eff}} = \frac{F^2 \eta_o}{1 + \frac{4}{\alpha + 3}\left(\frac{\tau_w}{\tau_{1/2}}\right)^{\alpha+1}} \tag{4}$$

The Ellis fluid model for the viscometric data (viscosity η vs shear stress τ) is:

$$\eta = \frac{\eta_o}{1 + (\tau_w + \tau_{1/2})^{\alpha-1}} \tag{5}$$

The factor F is a wall correction factor[53] due to the finite diameter, D_c, of the cylindrical chamber containing the beads.

$$F = 1 + \frac{4D_p\phi}{5D_c(1 - \phi)} \tag{6}$$

In the evaluation of η_{eff}, the wall shear stress, τ_w, was:

$$\tau_w = \frac{12D_p\phi}{150F(1 - \phi)} \frac{\Delta P}{L} \tag{7}$$

The superficial velocity, v, was obtained from the volumetric flow rate:

$$v = 4Q/\pi^2 D_c \tag{8}$$

Logarithmic plots of the Ergun coordinates $f \cdot \text{Re}$ vs Re were made. The Reynolds number for the onset of deviations were determined by two methods. In the first, a graphical extrapolation was made and Re_o determined from the intersection of the rising part of the polymer flow curve and the low Re section of the flow curve. We also determined numerically the inflection point of these $f \cdot \text{Re}$ versus Re plots using a spline-fitting routine. The qualitative trends were not changed by either choice. Characteristic values of the Reynolds number for onset determined using the first method were designated by Re_o. The inflection points were designated as Re*.

For the case of dilute solutions ($c[\eta] < 1$) we used the relations developed by Durst and co-workers[47,50] to make interpretations in terms of changes in molecular weights. The onset of the stretching transition was taken to occur at a value of the Deborah number De = 0.5. The Deborah number was defined as:

$$\text{De} = \tau \cdot \epsilon \tag{9}$$

The appropriate τ for the polymer was the first Rouse relaxation time:[54]

$$\tau = \frac{[\eta]\eta_s M}{\text{A}k_b T} \tag{10}$$

The intrinsic viscosity of the polymer, $[\eta]$, was determined from extrapolation of 4-bulb capillary viscometry data to zero shear rate and zero polymer concentration. The molecular weight of the HPAMs were calculated from $[\eta]$ using the Mark-Houwink coefficients ($[\eta] = KM_w^a$) given by Klein and Conrad.[55] It should be noted that the solvent used by Klein and Conrad was $0.5M$ NaCl, whereas it was $1M$ NaCl in this study. The solvent viscosity, η_s, was measured in capillary flow. The other parameters in Eq. 10 are A, Avagadro's constant, k_b, the Boltzmann constant, and T the absolute temperature. Marshall and Metzner[37] have shown the average elongation rate to be v/D_p for porous media. This made the nominal elongation rate:

$$\epsilon = \frac{k_1 v}{D_p} = \frac{k_1(1-\phi)\eta_{\text{eff}}\text{Re}}{D_p^2 \rho F} \tag{11}$$

The parameter k_1 can be determined experimentally[47] and has been seen to vary from $O(1)$ to $O(10)$ for various packed beds of spheres. We determined the best value of k_1 for our packed beds from:

$$k_1 = \lim_{c \to 0} \frac{D_p}{2\tau v_o} \tag{12}$$

where τ was from Eq. 10 and v_o was the superficial velocity at the onset of viscoelastic effects. Our best fit was for $k_1 = 4$.

One outcome of the above analysis is that:[50]

$$\text{Re}_o = \left\{ \frac{\rho_s \text{A} k_b T}{16\eta_s^2(1-\phi)(1+[\eta]c)K} \right\} \frac{D_p^2}{M^{(1+a)}} \tag{13}$$

for dilute solutions. The factor in curly brackets was only weakly dependent on polymer concentration, c, and this allowed us to use the proportionality:

$$M_w \sim \text{Re}_o^{(1+a)} \tag{14}$$

in investigating changes in molecular weights due to hydrodynamic degradation. It should be stressed again that this was valid only for dilute polymer solutions.

Hydrodynamic Degradation

To investigate the effect of high flow rates, similar to those encountered at the injection well in polymer flooding, polymer solutions were degraded in the glass bead pack at much higher flow rates than in the characterization experiments. Effluent was collected when a constant average pressure drop across the porous medium was achieved. In all cases the pressure drop at these higher flow rates fluctuated about a mean, even with a steady reservoir pressure. The fluids both before and after degradation were characterized viscometrically over a shear rate range of 0.1–300 sec^{-1} in a Haake RV100/CV100 rheometer as well as in the porous media rheometer. In some

TABLE I
Polymer Characteristics

	HPAM 1	HPAM 2
$[COO^-]$ (mol%)	30	13
$[\eta]$; 25.0°C/1M NaCl (dL/g)	28.0	26.3
M_w; viscometric (megadaltons)	6.1	8.5
M_w; Eq. (13) (megadaltons)	17.8	12.9
$c^* = 1/[\eta]$(ppm)	357	380
Mark-Houwink coefficients[55]:		
$K(10^{-4}$dL/g)	0.65	0.64
a	0.83	0.81

experiments the fluids were diluted to 50 ppm polymer concentration prior to characterization in the porous medium. Typically the polymer solutions passed through about 3.6 cm of bead pack ($\sim 60\ D_p$) in a single pass. To determine whether the amount of hydrodynamic degradation had reached a steady state after 1 pass we ran multiple passes on several samples. For flow rates up to several times those used in the rest of the degradation experiments there was no appreciable difference between 1 and 3 passes through the porous medium.

Polymer Solutions

Two samples of poly(acrylamide-co-sodium acrylate) were prepared by radical polymerization and subsequent hydrolysis. The carboxylate content was determined with infrared spectroscopy. Polymer samples were dissolved by rolling 0.2–0.3 wt% samples in distilled deionized filtered (0.2 μm Millipore) water in glass jars with polyethylene-lined caps for 1–2 days. The solutions were then diluted, the pH adjusted to 7.5 with HCl/NaOH and enough water and NaCl added to result in a final stock solution of 0.1 wt% polymer in 1M NaCl. This was then slowly filtered through an 8 μm Nuclepore filter (several hours for 1 liter). Both porous media and viscometric rheological characterizations before and after filtration showed no evidence of polymer degradation in this process. All dilutions were made with filtered (0.8 μm Nuclepore) 1M NaCl. The parameters characterizing the polymers are shown in Table I.

Additional Considerations

A number of phenomena other than non-Newtonian viscometric and viscoelastic effects can contribute to the flow behavior of polymer solutions in porous media. We designed our experiments to eliminate or mitigate most of these in order to focus on the viscous and elongational components to flow resistance and thus simplify the analysis of polymer concentration effects on hydrodynamic degradation. Chauveteau[42] has discussed most of these additional factors. They include polymer adsorption, hydrodynamic retention, depletion layer effects, pore size effects on permeability and mobility, and unsteady flows. We chose a packed bed of large glass beads to reduce the first five effects. Chauveteau[56] showed for xanthan polysaccharide (a stiff macro-

molecule) solution flow through glass bead packs that the effects of the depletion layer became constant and negligible for bead diameters > 200 microns. This was based on the bead size dependence of a constant relating shear rate to average fluid velocity. For our experiments the ratio of bead diameter to polymer radius of gyration was > 1000 and we expected negligible depletion layer effects. Also these effects would be most noticeable in the Newtonian regime. All of our Re_0 for viscoelastic effects, upon which our polymer degradation and characterization depended, were beyond the Newtonian regime. The mean hydraulic radius was > 100 times the average polymer radius of gyration and we expected adsorption effects to be minimized. Hydrodynamic retention could not be completely ruled out. Unsteady flows were expected to produce fluctuations in ΔP and these were seen, but usually at Re values higher than the Re_0 for viscoelastic effects. This unsteadiness became more pronounced at higher polymer concentrations.

RESULTS AND DISCUSSION

Polymer solutions were characterized both viscometrically and in porous media flow at various concentrations before hydrodynamic degradation. Figure 3 shows a typical modified Ergun plot for HPAM 2 at different polymer

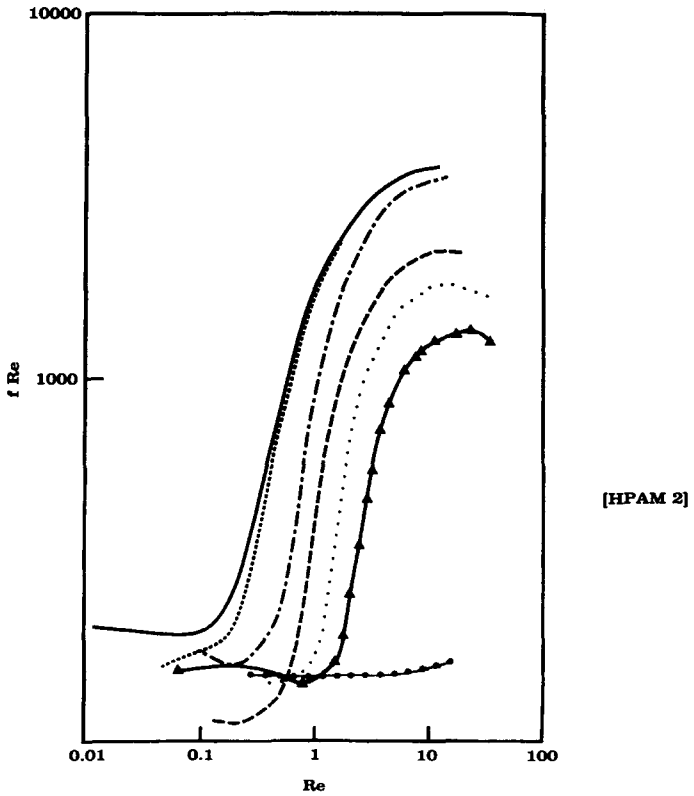

Fig. 3. Resistance factor vs. Reynolds number; 0–1000 ppm HPAM 2 in 1*M* NaCl: (● – ● – ●) 1*M* NaCl; (▲-▲) 50 ppm; (· · ·) 100 ppm; (– – –) 200 pm; (- – -) 400 ppm; (- - -) 750 ppm; (—) 1000 ppm.

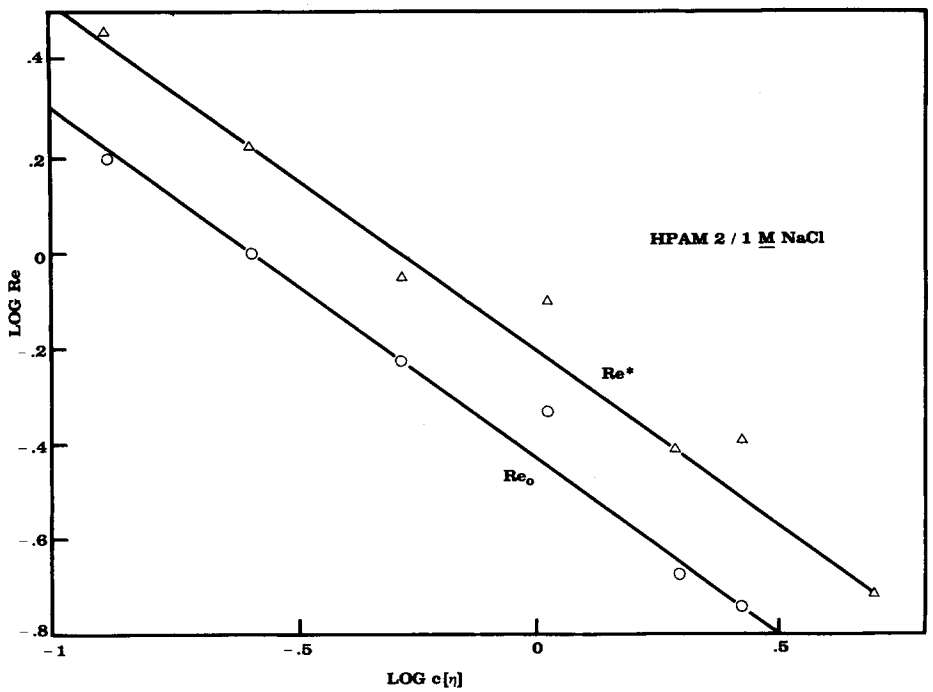

Fig. 4. Log–log plot of onset (Re_o) and inflection point (Re*) Reynolds numbers vs. $c[\eta]$ for HPAM 2 in 1M NaCl.

concentrations. The curve for 1M NaCl was a horizontal line beginning to deviate upward at a Reynolds number of about 10 as expected. The polymer solution curves demonstrated the onset of an excess resistance to flow at an onset Reynolds number, Re_o, which decreased with increasing polymer concentration. For the lower concentrations the curves reached a maximum and began to decline at the higher Reynolds numbers, indicating a flow regime where measurable hydrodynamic degradation was taking place. The overlap concentration, $c^* = 1/[\eta]$, for the polymer in Figure 3 was 380 ppm.

According to Eq. (14), $Re_o \sim 1/M_w^{(1+a)}$ for dilute solutions. Since our samples did not span an appreciable molecular weight range we correlated Re_o with the Simha parameter,[57] $c[\eta]$, shown on a log–log plot in Figure 4. A linear correlation persisted even for $c[\eta] > 1$. Plotting Re*, which was the Reynolds number at the inflection point of the modified Ergun plot, versus $c[\eta]$ on the same log–log plot also resulted in a linear correlation with nearly the same slope as with Re_o.

Molecular weights calculated from Eq. (13) are listed in Table I. These molecular weights were quite a bit higher than those predicted from the Mark-Houwink coefficients we used (see Table I). Recall that these coefficients were from data measured in 0.5M NaCl. Using the same values at 1M NaCl would tend to overestimate the molecular weights, especially for HPAM 1 which was more anionic. Our samples were also expected to be quite polydisperse. The larger values of the molecular weights derived from the onset of the excess pressure drops for a broad distribution would be expected since the higher molecular weight components would be stretched at a lower Reynolds number than components of the mean molecular weight.

Miles and Keller[58] have investigated the dynamics of dilute polymer solutions in elongational flow in a crossed slot device using the birefringence induced in the solution upon macromolecular extension to monitor this process. The derivative of the birefringence, Δn, versus strain rate, ϵ, resulted in a curve proportional to the mass distribution of the polymer. In a similar sense, locating the inflection points on the modified Ergun plots ($\delta^2(f \cdot \mathrm{Re})/\delta^2\mathrm{Re} = 0$) located the critical Reynolds number corresponding to the median in the mass distribution. It might be argued that such a choice would be more appropriate for characterizing polymers with appreciably broad molecular weight distributions. In our experiments, interpretations based on Re_o and Re* paralleled one another.

The excess resistance to flow due to macromolecular extension after taking into account the non-Newtonian viscometric contribution was useful for porous media flow modeling studies. The Darcy viscosity,

$$\mu = \frac{k}{v}\frac{\Delta P}{L} \tag{15}$$

was composed of a viscometric and an excess term:

$$\mu(v) = \eta_{\mathrm{eff}}(\tau) + \eta_{\mathrm{ex}}(\epsilon) \tag{16}$$

η_{eff}, the viscometric term, was calculated from Eqs. (4) and (5). This allowed

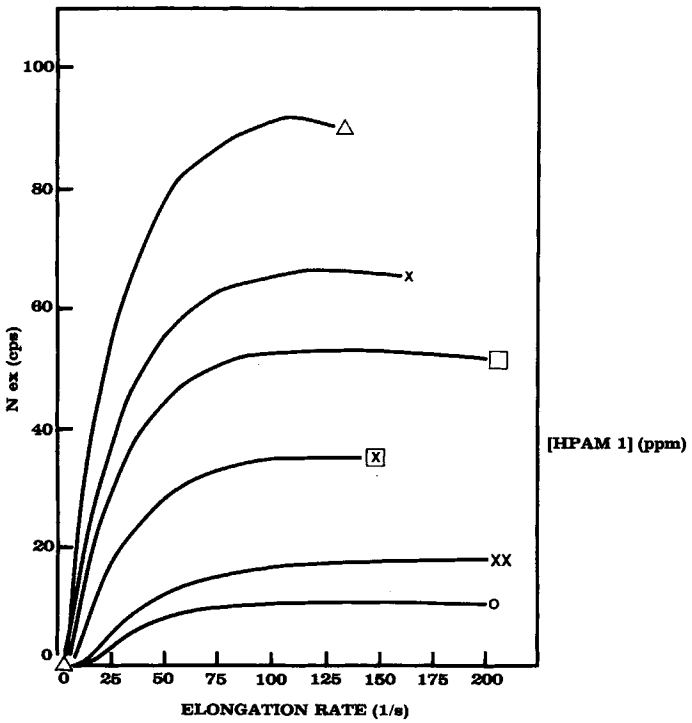

Fig. 5. Excess viscosity vs elongation rate in porous media flow for 50–1000 ppm HPAM 1 in 1*M* NaCl: (△) 1000; (×) 750; (□) 500; (⊠) 250; (××) 100; (○) 50.

us to extract η_{ex}. Sorbie and Roberts[59] modeled this excess viscosity as:

$$\eta^*_{ex}(v) = \eta_o[1 + D(v - v_o)]^x - \eta_o \tag{17}$$

where η_o was the zero shear rate viscosity of the polymer solution, D and x were constants and v_o was the superficial velocity at the onset of viscoelastic effects. Data for the excess viscosity of HPAM 1 solutions shown in Figure 5 suggested that an asymptotic analytical form was most appropriate for η_{ex}.

In the hydrodynamic degradation experiments an attempt was made to process the polymer solutions at different polymer concentrations at similar average elongation rates in the bead pack. The elongation rate was chosen as the independent variable, since for a given porous medium the amount of degradation has been shown to be proportional to the average elongation rate.[26,27,60] Chauveteau[42] used a capillary bundle model correlation for the average shear rate:

$$\dot{\gamma} = v\alpha_1/(k\phi/2)^{1/2} \tag{18}$$

where the parameter α_1 was taken to be 1.7 for large diameter beads. The elongation rate calculated with Eq. 11 was also proportional to the average

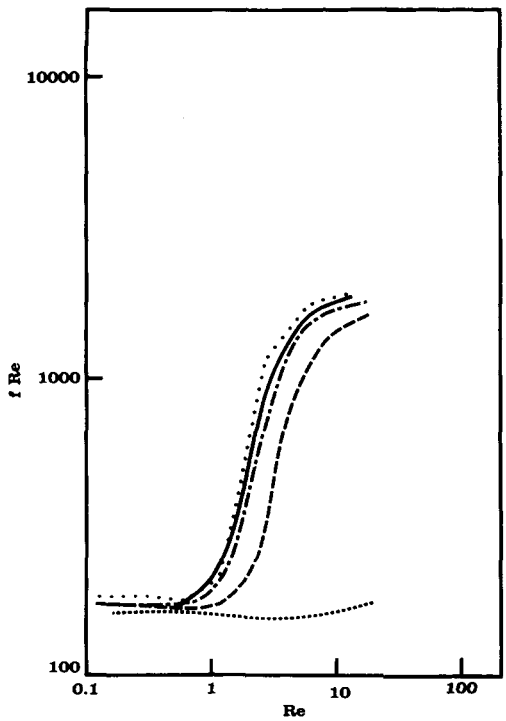

Fig. 6. Resistance factor vs. Reynolds number for HPAM 1 in 1M NaCl degraded at 750 ppm at various strain rates, $\dot{\epsilon}_{deg}$, then characterized at 50 ppm in the porous media rheometer: (- - -) 1M NaCl; (· · ·) 0; (—) 35; (– – –) 58; (– – –) 110 sec^{-1}.

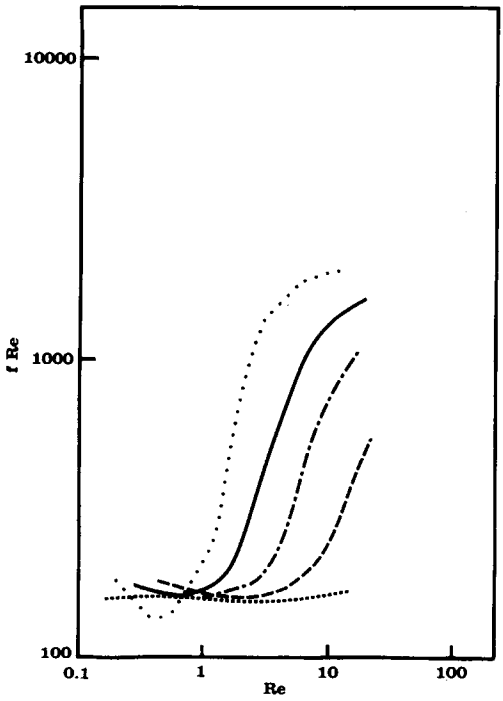

Fig. 7. Resistance factor vs. Reynolds number for HPAM 1 in 1*M* NaCl degraded at 100 ppm at various strain rates, $\dot{\epsilon}_{deg}$, then characterized at 50 ppm in the porous media rheometer: (- - -) 1*M* NaCl; (· · ·) 0; (—) 28; (- - -) 59; (– – –) 94 sec^{-1}.

shear rate in the porous medium since in this simple approximation they were both linearly related to the superficial velocity. Thus we have:

$$\dot{\epsilon} = \frac{k_1(k\phi/2)^{1/2}\dot{\gamma}}{\alpha_1 D_p} \tag{19}$$

Figures 6 and 7 show the modified Ergun plots for HPAM 1 characterized at 50 ppm after hydrodynamic degradation at 750 and 100 ppm ($c^* = 380$ ppm). Since the elongation rates, $\dot{\epsilon}_{deg}$, during the degradation phase were similar, it was obvious from these plots that a greater amount of change had occurred in the 100 ppm sample.

Figure 8 is a plot of Re_o versus $\dot{\epsilon}_{deg}$ for HPAM 1. Each solution at a specific polymer concentration experienced hydrodynamic degradation in the bead pack at a superficial velocity of $(D_p \cdot \dot{\epsilon}_{deg}/k_1)$. Each solution was then diluted to 50 ppm and characterized at lower velocities in the beadpack. The Re* values were taken from the inflection points of spline fits of the modified Ergun plots for each of these diluted solutions. These data are plotted as $Re^{*-(1/1+a)}$ versus $\dot{\epsilon}_{deg}$ in Figure 9. The ordinate in Figure 9 is proportional to the polymer molecular weight. This parameter decreased linearly with $\dot{\epsilon}_{deg}$

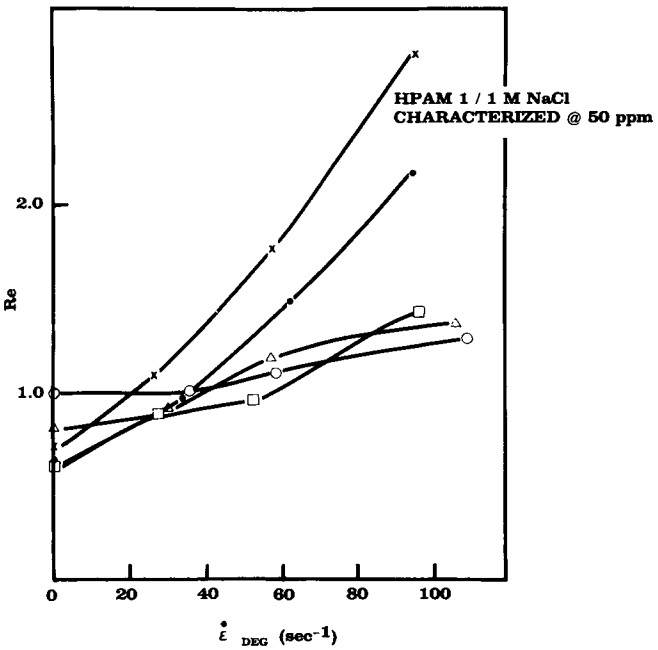

Fig. 8. Onset Reynolds number, Re_o, vs. degradation strain rate for 100–1000 ppm HPAM 1 in 1*M* NaCl. Re_o values derive from measurements of postdiluted (to 50 ppm) samples after degradation: (□) 1000 ppm; (○) 750 ppm; (△) 500 ppm; (×) 250 ppm; (·) 100 ppm.

in accord with observations of other investigators.[26,28] The data in both Figures 8 and 9 break up distinctly into two groupings, one for low polymer concentrations and one for higher polymer concentrations. In the cases we have studied so far, a significant difference in the amount of hydrodynamic degradation occurred depending on whether the polymer solutions were significantly above or below c^*. This suggested a difference in the dynamics of hydrodynamic degradation for different polymer concentration regimes. When the hydrodynamic degradation was a result of elongational flow, the loss of molecular weight was more severe for dilute solutions at equivalent superficial velocities, all else being equal.

The assumption from dilute solution theory which broke down first as higher polymer concentrations were encountered was the linear dependence of $\dot{\epsilon}$ solely on v/D_p; [Eq. (11)]. Direct determinations of the velocity field in converging flow[45] and in a crossed slot device,[61] both of which have strong elongational components, have shown that $\dot{\epsilon}$ is a complicated function of v as the polymer begins to interact with the flow field.

Inertial effects in the flow must also be considered when analyzing pressure drop/flow rate data. As Deiber and Schowalter[44] pointed out, the onset of viscoelastic effects in tubes with axial sinusoidal variations can occur before any secondary flows. We have associated this viscoelastic behavior with the excess pressure drops above and near Re_o. However, at higher Reynolds numbers secondary flows become important. We have associated this inertially dominated behavior with pressure fluctuations under steady superficial velocity. In a detailed study of extensional flow of dilute poly(ethylene oxide)

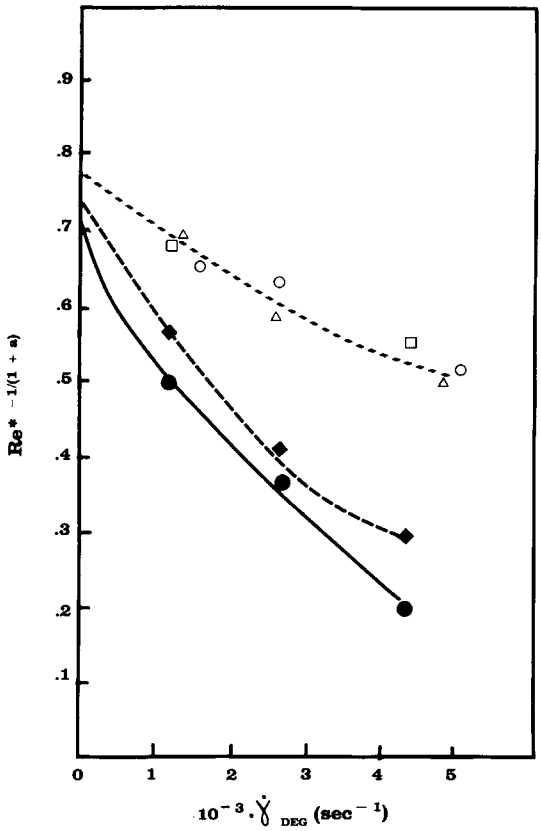

Fig. 9. Molecular weight parameter, Re*, vs. degradation shear rate for 100–100 ppm HPAM 1 in 1*M* NaCl. Re* values derived from measurements of post-diluted (to 50 ppm) samples after degradation: (□) 1000 ppm; (○) 750 ppm; (△) 500 ppm; ◆ 250 ppm; (●) 100 ppm.

solutions in converging channels James and Saringer[62] reported that above a critical extension rate there was an abrupt change in the flow pattern "from a simple converging motion to one dominated by a large unsteady vortex ring surrounding the channel opening on the upstream side". A cyclic motion of this vortex sometimes produced large pressure drop fluctuations. Once this secondary motion had started, the channel geometry seemed to no longer influence the central flow pattern which would become more confined to a conical volume associated with the vortex ring. Increasing polymer concentration exacerbated these non-Newtonian effects. These pressure fluctuations necessarily limit the reliable flow rate range for characterization and can be missed with manometric measurements.

The appearance of these effects and the generally complex relationship between $\dot{\epsilon}$ and v made it more difficult to extract polymer relaxation times and molecular weight information from the flow curves via Eqs. (9) and (13), respectively. This still can be possible for nondilute solutions, however, if either $\dot{\epsilon}$ is determined directly or can be calculated for an appropriately simple geometry by a theory which includes viscoelastic effects.

CONCLUSIONS

Porous media rheometry was used to monitor molecular weight changes due to hydrodynamic degradation in a glass bead pack. At equivalent superficial velocities, high molecular weight poly(acrylamide-co-sodium acrylate) polymers in dilute solutions in 1*M* NaCl experienced a greater loss of molecular weight in porous media flow than these polymers at semidilute concentrations. The results suggested a different concentration dependence of polymer degradation for concentrations above and below the overlap concentration. Based on the relative slopes in Figure 9 for the two groupings of hydrodynamic degradation data, the molecular weight loss at a given set of flow conditions was three times as great for the dilute solutions than for the semidilute solutions.

We would like to thank Prof. R. K. Prud'homme for his encouragement, insight, and helpful suggestions during the course of this project. We also acknowledge the helpful comments of Dr. G. Chauveteau in the preparation of this manuscript.

References

1. D. W. Schaefer, *Polymer*, **25**, 387 (1984).
2. P. G. de Gennes, *Scaling Concepts in Polymer Physics*, Cornell University Press, New York, 1979.
3. M. Daoud, J. P. Cotton, B. Farnoux, G. Jannink, G. Sarma, H. Benoit, R. Duplessix, C. Picot, and P. G. de Gennes, *Macromolecules*, **8**, 804 (1975).
4. S. F. Edwards, *Proc. Phys. Soc.*, **88**, 265 (1966).
5. M. A. Moore, *J. Phys. (Paris)*, **38**, 256 (1977).
6. M. Muthukumar, *J. Chem. Phys.*, **79(8)**, 4048 (1983).
7. M. Muthukumar and K. Freed, *Macromolecules*, **11(5)**, 843 (1978).
8. C. J. T. Martel, T. P. Lodge, and J. L. Schrag, "Initial Concentration Dependence of the Oscillatory Flow Birefringence and Viscoelastic Properties of Polymer Solutions", Proc. IUPAC 28th Macromol. Symp., Univ. of Massachusetts, Amherst, 864 (1982).
9. T. P. Lodge, J. W. Miller, and J. L. Schrag, *J. Polym. Sci., Polym. Phys.*, **20**(8), 1409–1425 (1982).
10. R. E. Harrington and B. H. Zimm, *J. Phys. Chem.*, **69(1)**, 161–175 (1965).
11. R. E. Harrington, *J. Polym. Sci., A-1*, **4**, 489–510 (1966).
12. Y. Minoura, T. Kasuya, S. Kawamura, and A. Nakano, *J. Polym. Sci., A-2*, **5**, 125–142 (1967).
13. W. Nagashiro and T. Tsunada, *J. Polym. Sci.*, **21**, 1149–1153 (1977).
14. A. H. Abdel-Alim, S. T. Balke, and A. E. Hamielec, *J. Appl. Polym. Sci.*, **17**, 1431–1442 (1973).
15. A. H. Abdel-Alim and A. E. Hamielec, *J. Appl. Polym. Sci.*, **17**, 3769–3778 (1973).
16. A. M. Basedow, K. H. Ebert, and H. Hunger, *Makromol. Chem.*, **180**, 411–427 (1979).
17. J. F. S. Yu, J. L. Zakin, and G. K. Patterson, *J. Appl. Polym. Sci.*, **23**, 2493–2512 (1979).
18. A. Ram and A. Kadim, *J. Appl. Polym. Sci.*, **14**, 2145–2156 (1970).
19. J. D. Cutler, K. G. Mayhan, G. K. Patterson, A. A. Sarmasti, and P. L. Zakin, *J. Appl. Polym. Sci.*, **16**, 3381–3385 (1972).
20. S. Ghoniem, G. Chauveteau, M. Moan, and C. Wolff, *Can. J. Chem. Eng.*, **59**, 450–454 (1981).
21. E. W. Merrill and P. Leopairat, *Polym. Eng. Sci.*, **20(7)**, 505–511 (1980).
22. E. W. Merrill and A. Horn, *Polym. Commun.*, **25**, 144–146 (1984).
23. R. L. Brennan and R. R. Jennings, *Polym. Preprints*, **22(2)**, 81–83 (1981).
24. J. A. Odell, A. Keller, and M. J. Miles, *Polym. Commun.*, **24**, 7–10 (1983).
25. J. M. Maerker, *S.P.E.* No. 5101 (1974).
26. J. M. Maerker, *Soc. Pet. Eng. J.*, **15**, 311–322 (1975).
27. R. S. Seright, *S.P.E.* No. 9297 (1980).
28. R. S. Seright, J. M. Maerker, and G. Holzwarth, *Polym. Preprints*, **22**(2), 30–33 (1981).

29. F. D. Martin, SPE/DOE 12651, Proc. SPE/DOE 4th Symp. Enhanced Oil Rec., April 1984, Tulsa, OK, vol. 1, 209 (1984).
30. E. W. Merrill and A. F. Horn, *Nature*, **312(5990)**, 140–141 (1984).
31. C. W. Morris and K. M. Jackson, *SPE* No. 7064, 5th Symp. for Improved Oil Recovery, SPE/AIME, Tulsa, OK (1978).
32. M. Barboza, C. Rangel, and B. Mena, *J. Rheol.*, **23(3)**, 281–299 (1979).
33. M. R. Mackley, *J. Non-Newtonian Fluid Mech.*, **4**, 111–136 (1978).
34. D. R. Oliver and R. Bragg, *Can. J. Chem. Eng.*, **51**, 287–290 (1973).
35. M. Van Dyke, *An Album of Fluid Motion*, Parabolic Press, Stanford, CA, 1982.
36. J. G. Savins, *Ind. Eng. Chem.*, **61**, 18–47 (1969).
37. R. J. Marshall and A. B. Metzner, *Ind. Eng. Chem. Fund.*, **6(3)**, 393–400 (1967).
38. H. C. Park, M. C. Hawley, and R. F. Blanks, *Polym. Eng. Sci.*, **15(11)**, 761–773 (1975).
39. T. J. Sadowski and R. B. Bird, *Trans. Soc. Rheol.*, **9(2)**, 243–250 (1965).
40. J. L. Duda, S. A. Hong, and E. E. Klaus, *Ind. Eng. Chem. Fund.*, **22**, 299–305 (1983).
41. P. G. de Gennes, *J. Chem. Phys.*, **60**, 5030 (1974).
42. G. Chauveteau, *S.P.E.* No. 10060 (1981).
43. G. Chauveteau, M. Moan, and A. Magueur, *J. Non-Newtonian Fluid Mech.*, **16**, 315 (1984).
44. J. A. Deiber and W. R. Schowalter, *A.I.Ch.E. J.*, **27(6)**, 912–920 (1981).
45. N. T. Hoa, G. Chauveteau, R. Gaudu, and D. Anne-Archard, *C.R.A.S. Ser. 2*, **294**, 927–932 (1982).
46. R. B. Bird, O. Hassager, R. C. Armstrong, and C. F. Curtiss, *Dynamics of Polymeric Liquids*, vol. 2, Wiley and Sons, New York, 1977.
47. R. Haas and F. Durst, *Rheol. Acta*, **21**, 566–571 (1982).
48. R. Haas, F. Durst, and W. Interthal, *Proc. Euromech.*, **143**/Delft, 163–168 (1981).
49. F. Durst, R. Haas, and B. U. Kaczmar, *J. Appl. Polym. Sci.*, **26(9)**, 3125–3149 (1981).
50. W. M. Kulicke and R. Haas, *Ind. Eng. Chem. Fund.*, **23**, 308–315 (1984).
51. R. Haas and W. M. Kulicke, *Ind. Eng. Chem. Fund.*, **23**, 316–319 (1984).
52. R. B. Bird, W. E. Stewart, and E. N. Lightfoot, *Transport Phenomena*, Wiley, New York, 1960.
53. D. Mehta and M. C. Hawley, *Ind. Eng. Chem. Proc. Des. Dev.*, **8**, 280 (1969).
54. G. Chauveteau and M. Moan, *J. Phys. Lett.*, **42**, 201 (1981).
55. J. Klein and K. D. Conrad, *Makromol. Chem.*, **179**, 1635–1638 (1978).
56. G. Chauveteau, *J. Rheol.*, **26(2)**, 111–142 (1982).
57. W. Graessley, *Adv. Poly. Sci.*, **16**, 125 (1974).
58. M. Miles and A. Keller, *Polymer*, **21**, 1295 (1980).
59. K. S. Sorbie and L. J. Roberts, "A Model for Calculating Polymer Injectivity Including the Effects of Shear Degradation," Atomic Energy Establishment, Winfrith, Dorchester, Dorset, England; Report AEEW-R1626 (1983).
60. J. M. Maerker, *Soc. Pet. Eng. J.*, **Aug.**, 172–174 (1976).
61. K. Gardner, E. R. Pike, M. J. Miles, A. Keller, and K. Tanaka, *Polymer*, **23(10)**, 1435 (1982).
62. D. F. James and J. H. Saringer, *J. Non-Newtonian Fluid Mech.*, **11**, 317–339, (1982).

Received April 11, 1986
Accepted September 5, 1986